Discharge through a Permeable Rubble Mound Weir

Michioku, Kohji
Maeno, Shiro
Furusawa, Takaaki
Haneda, Masanori

(Citation)
Journal of Hydraulic Engineering,131(1):1-10

(Issue Date)
2005-01

(Resource Type)
journal article

(Version)
Accepted Manuscript

(URL)
https://hdl.handle.net/20.500.14094/90000999

DISCHARGE THROUGH A PERMEABLE RUBBLE MOUND WEIR

Kohji Michioku[1], *Shiro Maeno*[2], *Takaaki Furusawa*[3] *and Masanori Haneda*[4]

ABSTRACT

The hydrodynamics of a rubble-mound weir are theoretically and experimentally examined. This type of weir is considered to be environmentally-friendly, since its permeability allows substances and aquatic life to pass through longitudinally. By performing a one-dimensional analysis on a steady non-uniform flow through the weir, discharge is described as a function of related parameters, such as flow depths on the up- and downstream sides of the weir, porosity and grain diameter of the rubble mound, weir length, etc. A laboratory experiment is carried out to determine the empirical coefficients included in the analytical model. The theoretical solution of the discharge is compared with the experimental data to verify the analysis. It is confirmed that agreement between theory and experiment is satisfactory for a wide range of flow conditions. The present study makes it possible to apply the rubble mound weir for practical use as a discharge control system.

CE Database subject headings: Weirs; Open channel flow; Permeability; Rockfill structures; Porous media flow; Discharge coefficients.

[1] Professor, Dept. of Civil Engin., Kobe Univ., 1-1 Rokkodai, Nada, Kobe 657-8501, Japan (corresponding author). E-mail: michioku@kobe-u.ac.jp

[2] Associate Professor, Dept. of Environ. Design and Civil Engin., Okayama Univ., 3-1-1 Tsushima-naka, Okayama 700-8530, Japan. E-mail: maeno@cc.okayama-u.ac.jp

[3] Engineer, Construction Technology Institute CTI Co. Ltd., 2-31 Hachobori, Nakaku, Hitorsima 730-0013, Japan. E-mail: furusawa@ctie.co.jp

[4] Engineer, Hanshin Railway Co. Ltd., 116 Kitashirouchi, Amagasaki 660-0826, Japan. E-mail: haneda.m@her.hanshin.co.jp

Keywords: weirs, discharge, rubble-mound, open channel flow, porous media flow, one dimensional analysis, near-nature river work

INTRODUCTION

A conventional weir typically consists of an impermeable body constructed of concrete, metal, rubber, etc., since its primary functions are to collect water and efficiently regulate river flow. However, an impermeable body prevents the longitudinal movement of aquatic life and transportation of physical and chemical substances in water, eventually having a negative impact on the river environment. Fig. 1 shows an example of traditional rubble mound weirs in Japan, which are used for irrigation. They were constructed many years ago, and a few of them are still preserved by local communities.

The rubble mound weir allows the streamwise migration of aquatic life, because the body is porous and the slope on the downstream side is mild. Pores, concavities and convexities on the granular slope surface allow aquatic animals to crawl and swim up the structure. In this manner, the structure may also serve the function of fish ladder or fish way. Minor modifications to the structure, such as the installation of a mild slope spillway, are expected to improve its performance as a fish ladder. From the viewpoint of water quality, physical and chemical substances such as sediments and suspended organic matter can pass downstream through the permeable body. This eventually minimizes sedimentation and eutrophication in an impoundment. Inside the rubble mound, bacteria inhabiting the granular surface may decompose organic matter. This biochemical reaction contributes to the purification of river water as it flows through the rubble mound, just like in water purification and sewage water plants. It is also expected that turbulence generated in the granular media will promote aeration through the air-water interface, helping in the aerobic decomposition of organic matter. In these respects, the rubble mound weir might be a structure with minimal negative impact on the river environment, and is considered to be more environmentally-friendly than most of the recently constructed impermeable weirs.

Knowledge of the hydrodynamic properties of the rubble mound weir is required for practical application, although little is still known regarding this type of structure. The authors' intention is to investigate the weir's performance as a water use facility, not as a flood control structure. Therefore, water storage and through-flow capacities of the weir in low water level are of interest to us. Events during a flood, such as failure of the weir against flow, local scouring around the weir, etc., are not included as subjects of this paper. Although there is an urgent need to investigate these subjects for engineering use of the weir, we can extend our research in this direction only after examination of the through-flow properties.

The objective of the study is to formulate discharge through the weir as a function of parameters such as water depth, porosity and rubble grain diameter, geometrical dimension of the structure, etc. A

one-dimensional analysis on a steady non-uniform flow around the rubble mound was performed to obtain strict theoretical solutions for water surface profile and discharge, in which laminar and turbulent components of flow resistance in the porous body were taken into consideration. A laboratory experiment was carried out to verify the analysis, in which a rectangular weir model was installed in an open-channel flume. A "discharge-curve", i.e. a functional relationship between discharge and water level, deduced from the analysis was compared with the experimental data to verify the analysis. The authors intend to establish the present theory as a guideline for the design of a rubble mound weir.

PREVIOUS WORK

In order to analyze flow through the rubble mound weir, we need the hydrodynamics both on a granular media flow and on a rapidly varied open channel flow around a weir. Theoretical descriptions of the latter have already been established and can be referred to mostly in well-known publications such as Chow (1959), French (1986), etc. Focus in this section is mainly placed on reviewing the former subject. General information on porous media flows is given in textbooks; for example, Stephenson (1979), Todd (1960) and Vafai (2000).

Since the rubble mound weir is to be designed as a discharge control facility in a river channel, the structure is installed in running water. Therefore, inertia force in the media is not negligible compared to hydraulic gradients and flow resistance. In addition, turbulence must be predominant. Arbhabhirama and Dinoy (1973), Basak (1977), Venkataraman and Rama Mohan Rao (1998), and many other researchers investigated the dependency of flow properties on Reynolds number. It is confirmed from the previous studies that flow turbulence in the present study is fully developed, since the Reynolds number $R_w=Vl_w/\nu$ in our experiment always ranges greater than 2,000, where V is a bulk velocity, l_w is a characteristic length scale of media or the rubble's mean diameter, and ν is a fluid viscosity. In a prototype, R_w must be clearly much greater. Hence, Darcy's law is no longer valid for describing flow resistance.

Commonly used non-Darcian resistance laws in the literature are grouped under two broad forms, a quadratic type and a power type, as

$$I = A_1 V + A_2 V^2 \tag{1}$$

$$I = A_3 V^W \tag{2}$$

where $I=-(dp/dx)/\rho g$ is the hydraulic gradient, (dp/dx) is the pressure gradient in the flow direction, ρ is the fluid density and g is the gravity acceleration. W and (A_1, A_2, A_3) are empirically or theoretically determined constants. Eq. (1) is a well known Forchheimer relation. Eq. (2) is the so-called Izbash equation. George

and Hansen (1992) proposed a conversion method between Eqs. (1) and (2), because both equations are convenient in different fields of engineering practice. Trussell and Chang (1999) provided a review of non-linear flow resistance laws Eqs. (1) and (2), and summarized their performance in the flow analysis. They pointed out several problems to be investigated further, and provided guidelines that research in this discipline should work out in the future. However, the use of Eq. (2) seems to have declined in recent years.

Many researchers have worked to theoretically and experimentally determine functional dependencies of (A_1, A_2) in Eq. (1) on relating parameters. Ward (1964) is one of those who successfully used a dimensional argument and proposed the following equation:

$$I = \underbrace{\{\nu/(gK)\}U_S}_{D_L} + \underbrace{\{c/(g\sqrt{K})\}U_S^2}_{D_T} \quad . \tag{3}$$

Here, U_S is the macroscopic velocity or apparent velocity. K is the permeability of the porous body with a dimension of length squared, and c is a dimensionless coefficient related to drag force acting on a particle. D_L and D_T in Eq. (3) are the laminar and turbulent flow components of the flow resistance, respectively. In the absence of D_T, Eq. (3) becomes equivalent to Darcy's law. Ward (1964) experimentally obtained a value of c =0.55 for the transition range between laminar and turbulent flows. Ahmed and Sunada (1969) theoretically deduced the same functional form as Eq. (3) for turbulent porous media flow from volumetric integration of the Navier-Stokes equation. They recommended a relationship $c=l_w/(K)^{1/2}$ instead of using a constant value of c. Arbhabhirama and Dinoy (1973) performed an analysis and a laboratory experiment to find a relationship of Eq. (3) that would be applicable for any type of porous media. They argued that c was dependent on particle mean diameter d_m and porosity n, while it was originally treated as a constant coefficient in the study by Ward (1964). This is written as

$$c = f \cdot \left(d_m / \sqrt{K/n}\right)^{-3/2} \tag{4}$$

where f is a non-dimensional coefficient and identified to be f=100 from experiments conducted with various gravel materials. Using experimental data collected by Arbhabhirama and Dinoy (1973), Shimizu, Tsujimoto and Nakagawa (1990) assumed a linear functional relationship between the permeability K and the particle diameter d_m as

$$\sqrt{K} = e \cdot d_m \tag{5}$$

The least square correlation leads to e =0.028. Strictly speaking, K might also be dependent on other parameters such as pore structure, geometry of grain particles, etc. Nevertheless, Eq. (5) gives a good approximation within the range of previous experimental data. Venkataraman and Rama Mohan Rao (1998)

examined the resistance law Eq. (3) in a wide range of flow conditions. Thiruvengadam and Kumar (1997) and Venkataraman and Rama Mohan Rao (2000) modified the flow resistance law Eq. (3) so that it can be applied to flow through porous media with converging boundaries, where the hydraulic gradient varies in the streamwise direction. Legrand (2002) analyzed the flow resistance formula based on the capillary model established by Comiti and Renaud (1989). He found that, in terms of the two structural parameters of porous media, i.e. the pore diameter and tortuosity, a single equation could represent all data obtained from various experimental conditions. The capillary model may have an advantage in that the coefficients in Eq. (3) can be precisely formulated as functions of pore structure.

The coefficients and functional forms in Eqs. (3) through (5) have been identified through laboratory experiments that were carried out mostly using test columns filled with grain samples, where the flow was uniform and confined. Nevertheless, they were successfully applied to groundwater systems such as embankments, rockfills, unconfined aquifers, ditch drainage, etc. that are horizontally two-dimensional and bounded by a free surface. Examples of these applications are Volker (1969), Volker (1975), Basak (1976), Basak (1977), Mustafa and Rafindadi (1989), and Hansen, Garga and Townsend (1994). Hansen, Garga and Townsend (1994) introduced an effective hydraulic gradient in order to apply the flow resistance principles from test column experiments to a two-dimensional flow analysis. They formulated the effective hydraulic gradient as a function of geometrical dimensions and water depth of the embankment, and proposed a formula for computing through-flow discharge. In addition to groundwater problems, the non-linear resistance formula was applied to other engineering issues. In chemical engineering, turbulent porous media flows are found in many reactor systems. Antohe and Lage (1997) and Chan, Fue-Sang and Yovanovich (2000), for example, performed k-ε turbulence modelling for two- and three-dimensional flows in porous media. In both of the studies, drag force in the media was formulated by a quadratic-type resistance law.

Since a rockfill embankment has a similar mechanism as a rubble mound weir in some aspects, many findings from this field could be applied to the present rubble mound system. Li, Garga and Davies (1998) and Samani, Smani and Shaiannejad (2003) are examples of those who recently analyzed flow through a rockfill dam. The latter conducted a numerical analysis for steady and unsteady flow through rockfill dams by using an exponential relationship between Reynolds number and Darcy-Weisbach coefficient. It was demonstrated that a two-dimensional model could more precisely describe phenomena than a one-dimensional model. There are, however, some differences between rockfill dams and rubble mound weir systems; for example, a rockfill is associated with still water, while the weir is associated with running water. In most of the rockfill analyses,

water depths on the up- and downstream sides are used only as boundary conditions for computing the media flow. However, in the rubble mound weir, the inertia force may play an important role even in the mound body. In addition, flow modelling at sudden contraction from the open channel to the porous body and sudden expansion from the porous body to the open channel is a key point in the analysis that has to be very carefully taken into account.

Parkin, Trollope and Lawson (1966) discussed discharge through a rockfill dam and its structural stability against flow force. They computed discharge assuming that the hydraulic gradient has a constant value at an internal control section. Critical flow analysis will also be used in our discharge computation, but only in special cases when a critical condition arises at the downstream end of the weir. One point of difference from the rockfill problem is that a rubble mound system does not always have a control section. Resolving the problem in the rubble mound system requires momentum principles that connect the porous media flow with the open channel flow, as discussed later.

As mentioned above, another major difference between the present system and many groundwater problems is that inertial force due to flow accelerations is not small enough to be neglected. Bari and Hansen (2000) and Hansen and Bari (2002) are among those who employed a momentum equation with the inertia term for numerically analyzing a buried stream through mine waste dumps. They mainly focused on the water surface profile under a given discharge, and the computational domain was limited in the porous media. Rubble mound weir systems, on the other hand, consist not only of a porous media, but also of an open channel. It is also important to note that in the rubble mound weir problem, discharge is not a given condition, but an unknown variable to be solved. Solutions for both water surface profile and through-flow discharge in the present system are strictly theoretical, not numerical.

A number of studies have been conducted on stability and the failure mechanism of rockfills and embankments; for example, Ulrich (1987), Curtis and Lawson (1967), Parkin, Trollope and Lawson (1966), and Garga, Hansen, and Townsend (1995). Although the stability problem is also important from an engineering point of view, in this study the authors will mainly focus on the hydraulic features or through-flow capacity of the rubble mound weir. In other words, discussion in this study will concentrate on the weir's performance as a water use facility, and not as a flood control facility. Of course, the study should be extended to address the failure mechanism of the rubble mound structure, but only after additional examination of weir overflow.

WATER SURFACE PROFILE ANALYSIS

The stream runs over the top of the weir in the case of high flooding. In this situation, the dynamic stability of the structure against flow force is of major engineering interest. This problem is, however, beyond our scope as discussed above. Focus here is placed on ordinary flow conditions, where the water surface is submerged under the top. This situation is more predictable for water use.

In the analysis, the rubble mound weir is assumed to be rectangular for analytical simplicity, whereas a prototype weir requires a trapezoidal geometry with slope for dynamic stability. The model is two-dimensional and divided into the three regions, as shown in Fig. 2. The regions are (I) the cross section at x=0 where flow suddenly converges from the open channel to the porous body, (II) the reach between x=0~L in which the subsurface flow is gradually varied in the porous body, and (III) the cross section at the downstream end of the weir x=L where flow rapidly diverges from the porous body to the open channel. Here, L is the weir length.

Momentum principles are applied to each region in order to analyze the flow profile, as described below.

Momentum Balance in Region (I): the Upstream Boundary, x=0

Here, the flow suddenly converges around x=0 from an open channel pouring into the weir of porosity n. It is a reasonable assumption from a hydrodynamic point of view that the flow transition is analogous to a sudden contraction from a wide open-channel to a narrow one, since the so-called Hele-Shaw model is a conventional way to simulate a flow system in a porous media. Consider the rubble mound system in Fig. 3(a) equivalent to a complex Hele-Shaw system with a two-dimensional porosity of

$$\lambda = \sum_{k=1}^{N} b_k / B_0 \tag{6}$$

in Fig. 3(b), and furthermore to a sudden contraction system as shown in Fig. 3(c).

In the system of Fig. 3(c), momentum and continuity equations are written in the same way as a conventional analysis of suddenly contracted open channel (see French (1986) for an example). They are

$$\rho Q(\delta_1 U_1 - \delta_0 U_0) = \rho g B_0 h_0^2/2 - \rho g (B_0 - B_1) h'^2/2 - \rho g B_1 h_1^2/2 \tag{7}$$

$$Q = U_0 B_0 h_0 = U_1 B_1 h_1 \tag{8}$$

Here B is the channel width and Q is the volumetric flow rate. δ is the velocity correction factor, and h is the flow depth. The subscripts 0 and 1 refer to variables just on the up- and downstream sides of the cross section x=0 or x=0^- and 0^+, respectively. h' is the transition water depth between the cross sections x=0^- and 0^+.

Equate two-thirds of the porosity n in the rubble mound system with a two-dimensional porosity or the width ratio λ=B_1/B_0 in the sudden contraction system, in other words, λ=$n^{2/3}$. Setting h'=h_0 as in a conventional analysis method for sudden contraction, and combining Eqs. (7) and (8) together, yields the following:

$$\mathsf{F}_0^2 = \frac{\lambda^2 \gamma_1 \left(1-\gamma_1^2\right)}{2\left(\delta_1 - \delta_0 \lambda \gamma_1\right)} \tag{9}$$

Here, $\gamma_1=h_1/h_0$ and $\mathsf{F}_0=q/(gh_0^3)^{1/2}$ is a dimensionless discharge in Froude number form and $q=Q/B_0$ is discharge per unit-width.

Water Surface Profile in the Reach of x=0~L or Region (II)

Compared to the rapid flow transition around x=0, the longitudinal variation of flow in this reach is rather gradual. Now, Eq. (3) is applied to describe the flow resistance in the rubble mound weir, where the apparent velocity or the superficial velocity is defined as $U_S=q/h$. It is considered that gradient of the total energy loss, $d\{(U^2/2g)+h+z_0\}/dx$, is balanced by the hydraulic gradient I, where z_0 is the channel bed elevation. The relationship is then written as follows:

$$\frac{d}{dx}\left(\frac{U^2}{2g}\right) + \frac{dh}{dx} - i + \underbrace{\frac{\nu}{gK}U_S}_{D_L} + \underbrace{\frac{c}{g\sqrt{K}}U_S^2}_{D_T} = 0 . \tag{10}$$

Here, $U = q/nh$ is the seepage fluid velocity and $i=-dz_0/dx$ is the bed slope.

Eq. (10) gives a differential equation for the water surface profile $h(x)$ as

$$\frac{dh}{dx} = \frac{i - \{\nu/(gK)\}(q/h) - \{c/(g\sqrt{K})\}(q^2/h^2)}{1-(1/n^2)\{q^2/(gh^3)\}} \tag{11}$$

With reference to Fig. 2, Eq. (11) is integrated with respect to x with boundary conditions of

$$h=h_1 \quad \text{at} \quad x=0^+ \qquad \text{and} \qquad h=h_2 \quad \text{at} \quad x=L^- \tag{12}$$

Normalization of the solution with (h_0, q) finally leads to the following solution:

$$\gamma_1 - \gamma_2 + li = \frac{a}{2}\ln\left|\frac{\gamma_2^2 - a\gamma_2 - b}{\gamma_1^2 - a\gamma_1 - b}\right| + \frac{a^2/2+b}{\sqrt{a^2+4b}}\ln\left|\frac{(\gamma_1-\beta)(\gamma_2-\alpha)}{(\gamma_1-\alpha)(\gamma_2-\beta)}\right| - \frac{d}{\sqrt{a^2+4b}}\left\{\frac{1}{\alpha}\ln\left|\frac{\gamma_1(\gamma_2-\alpha)}{(\gamma_1-\alpha)\gamma_2}\right| - \frac{1}{\beta}\ln\left|\frac{\gamma_1(\gamma_2-\beta)}{(\gamma_1-\beta)\gamma_2}\right|\right\} \tag{13}$$

where

$$(\alpha,\beta) \equiv (a \pm \sqrt{a^2+4b})/2, \quad a \equiv \mathsf{F}_0^2/(ki\mathsf{R}e), \quad b \equiv (c\mathsf{F}_0^2)/(\sqrt{k}i), \quad d \equiv \mathsf{F}_0^2/n^2 \tag{14}$$

and $\gamma_j=h_j/h_0$ (j=1,2) is a dimensionless water depth, $\mathsf{R}_e=q/\nu$ is Reynolds number, $k=K/h_0^2=e(d_m/h_0)^2$ is a dimensionless length scale regarding the rubble grain diameter and $l=L/h_0$ is a non-dimensional weir length. Eq. (13) shows the dependency of discharge q on the water depths (h_1, h_2) as well as on the weir length L in an implicit functional form. This is written as

$$\phi(\mathsf{F}_0, \gamma_1, \gamma_2, l)=0 \tag{15}$$

where ϕ is a function corresponding to Eq. (13).

As seen in Eq. (13), other important dimensionless parameters included in Eq. (14) are Reynolds number R_e, porosity n, gravel diameter in dimensionless form d_m/h_0 and bed slope i.

Momentum Balance in Region (III): the Downstream Boundary, $x=L$

In this cross section, the stream suddenly diverges from the porous body to the open channel. The following two types of situations may arise depending on the downstream flow condition.

(a) "C-Flow": a flow regime in which discharge is controlled at the downstream edge of the weir, and the flow on the downstream side is supercritical

For a relatively small water depth at the downstream side of the weir, the flow is supercritical and the cross section $x=L^-$ becomes a discharge-control section. In this case, the depth h_2 is equated with a critical depth h_C at which the discharge Q is determined. Since flow in the weir is not influenced by the downstream condition, h_C is determined independently of the downstream water depth h_3 from a singularity condition of the differential equation (11). In other words, h_C is computed by equating the denominator in Eq. (11) to zero. The result is

$$h_C/h_0 = h_2/h_0 = \gamma_2 = (F_0/n)^{2/3} \quad . \tag{16}$$

The flow regime in this case is referred to as "C-Flow (flow is critical at $x=L$)" hereinafter.

(b) "S-Flow": a flow regime in which flow remains sub-critical throughout the entire reach

When sub-critical flow conditions are present on the downstream side of the weir, the flow is dammed up from downstream. The flow rate in this case is dependent not only on h_2 at $x=L^-$ but also on h_3 at $x=L^+$. Conservations of momentum and mass are formulated in the same manner as in the analysis for the cross section $x=0$, as

$$\rho Q(\delta_3 U_3 - \delta_2 U_2) = \rho g B_1 h_2^2/2 + \rho g(B_0 - B_1)h''^2/2 - \rho g B_0 h_3^2/2 \tag{17}$$

$$Q = U_2 B_1 h_2 = U_3 B_0 h_3 \tag{18}$$

where the subscripts 2 and 3 refer to variables on the up- and downstream sides of the cross section $x= L$ or $x=L^-$ and L^+, respectively. h'' is the transition water depth between $x=L^-$ and L^+. This is equated with h_0 as in an analysis for a sudden channel expansion.

Eqs. (17) and (18) show the functional dependency of discharge Q on the flow depths (h_2, h_3) as

$$F_0^2 = \frac{\lambda\gamma_3(\gamma_2^2 - \gamma_3^2)}{2\{\delta_3\lambda - \delta_2(\gamma_3/\gamma_2)\}} \quad , \tag{19}$$

where $\gamma_3 = h_3/h_0$.

This type of flow is downstream-controlled and is referred to as "S-Flow (flow is subcritical at $x=L$)" hereinafter.

COMPUTATION OF DISCHARGE

A solution for flow rate is obtained by combining the solutions for water surface profile in regions (I) through (III). This is done by eliminating (h_1, h_2) in Eqs. (9), (13), (16) and (19), which yields a solution for flow rate Q as a function of the water depths h_0 and h_3. This procedure is equivalent to the elimination of (γ_1, γ_2) in the normalized equation system, which gives a solution for the normalized discharge F_0 as a function of the dimensionless water depths (h_0/L, h_3/h_0). In computation, all the velocity correction factors δ_1, δ_2 and δ_3 are assumed to be unity. Solutions for the discharge are given for the two flow regime cases, i.e. the C-Flow and S-Flow, respectively, as shown below.

Discharge of C-Flow

Treating (γ_1, γ_2) as dummy variables in Eqs. (9), (13) and (16), F_0 is given as a function of h_0/L as

$$F_0 = \Omega_C(h_0/L) \tag{20}$$

where the function Ω_C is an implicit function given by Eqs. (9), (13) and (16).

Discharge of S-Flow

F_0 is correlated to the parameters h_0/L and $\gamma_3=h_3/h_0$ through Eqs. (9), (13) and (19). Here, a dimensionless water level difference $\Delta h/h_0[\equiv(h_0-h_3)/h_0=1-\gamma_3]$ is used instead of γ_3. The solution for the discharge is then given by

$$F_0 = \Omega_S(h_0/L, \Delta h/h_0) \tag{21}$$

where the functional form of Ω_S is determined from Eqs. (9), (13) and (19).

The parameter $\Delta h/h_0$ reflects the influence of the backwater from downstream. The smaller the water depth difference $\Delta h/h_0$, the more predominant the dam-up due to backwater. The discharge F_0 decreases as $\Delta h/h_0$ decreases. Eq. (21) asymptotically approaches Eq. (20) as $\Delta h/h_0$ increases or as the backwater effect decreases.

Governing Parameters

Considering the functional relationships included in Eqs. (20) and (21), the governing parameters that determine the flow rate are as follows:

(a) Reynolds number: $R_e=q/\nu$,

(b) Porosity of the rubble mound: n,

(c) Rubble grain diameter in dimensionless form: d_m/h_0,

(d) Channel bed slope: i.

LABORATORY EXPERIMENT

Laboratory experiments were carried out in two different open channel types, the “K-Flume”, i.e. the flume at Kobe University, and the “O-Flume”, i.e. the flume at Okayama University. The length, height and width of the K-Flume were 7.0m×0.2m×0.45m, and those of the O-Flume were 5.0m×0.6m×0.4m. The O-Flume reproduced relatively large-scale flows with R_e>5,000. In this range, the flow properties were approximately independent of Reynolds number and thus the scale effect of the model was negligible, as discussed later. On the other hand, the flow in the K-Flume was relatively small and flow was eventually influenced by viscosity or by Reynolds number. In both experiments, a rectangular rubble mound was installed in the channels and reinforced with a wire net so that the mound would not collapse due to the flow.

Natural round gravel with two different mean diameters d_m were used as rubble mound materials, but the resultant porosity n of the two cases did not differ significantly. This suggests that, in the case of the present rubble mound materials, the pore structure is not greatly influenced by the grain diameter d_m and thus the permeability K might be dependent mainly on d_m as assumed in Eq. (5). Fig. 4 shows the cumulative size-distribution curves for the two materials that were obtained from the experiment in the K-Flume. They are larger than the materials used in the study of Arbhabhirama and Dinoy (1973) in which the mean particle diameter ranged between d_m=0.54~16.1mm. Approximately uniform distributions of diameter can be assumed for both cases. The experiments were conducted for various ranges of weir length L, bed slope i, Reynolds numbers and Froude numbers. In both experiments, discharge was measured by a V-notch orifice, and water surface profile was obtained from a point gauge. Because the O-Flume's V-notch orifice was small, there was an undesirable oscillation of water surface that prevented us from making a precise measurement of discharge. We tried to take an average of the fluctuating water depth, but it should be noted that uncertainty still remained in the discharge measurement. This problem will be discussed in more detail later. The experimental conditions for the K-Flume experiment and the O-Flume experiment are listed in Tables 1 and 2, respectively. Discharge Q and downstream water depth h_3 vary under a given model condition, and about ten to twenty experimental runs were performed in each combination of (d_m, L, i). The total number of experimental runs or data points were M_K=246 for the K-Flume experiment, and M_O=99 for the O-Flume experiment, as listed in row (5) of Tables 1 and 2.

DETERMINATION OF THE UNKNOWN COEFFICIENTS (e, f)

The most important step in the analysis is the formulation of the flow resistance in Eq. (10). There is no

guarantee that the coefficients (e, f) from the previous studies are suitable to the present flow system; they were determined from the experiments on confined porous media flows with no spatial flow acceleration, while the present flow system is a spatially varied porous-media flow bounded by a free water surface.

Now, the coefficients are determined so that square sum of error between the experimental and theoretical discharges

$$\varepsilon(e, f) = \sum_{m=1}^{M_K+M_O} \{Q_m^{th}(e, f) - Q_m^{ex}\}^2 \qquad (\mathrm{m}^6/\mathrm{sec}^2) \tag{22}$$

is minimized. Here, Q_m^{ex} is a discharge from an experimental run m and $Q_m^{th}(e, f)$ is the corresponding theoretical discharge computed for the pair (e, f). Note that the total number of experimental runs was M_K+M_O = 246+99=345, as shown in Tables 1 and 2.

Contours of the error ε are drawn in Fig. 5 for varied combination of (e, f). From the figure, the optimum values of the coefficients giving the minimum error are identified as (e, f)=(0.0196, 41.0). They are in the same order as the values found in the literature, i.e. (e, f)=(0.028, 100). However, we need to pay attention to their discrepancies, because the solution is somewhat dependent on (e, f). There are two possible reasons for discrepancy. The first possible reason for discrepancy may be due to the difference in the flow systems; (e, f)=(0.028, 100) were obtained from porous-media flows in confined test columns, while the present system, which provides (e, f)=(0.0196, 41.0), is an unconfined porous media flow connected to an open channel. The second possible reason for discrepancy is the uncertainty in Eqs. (3) through (5). A recent study by Legrand (2002) suggests that the coefficients (e, f) may depend on the pore structure in the media, while they are assumed to be constant in the present analysis. Further investigation is, of course, required in order to find the exact values of (e, f). However, the authors' interest is in analyzing streamwise flow structure and computing discharge, rather than in strictly formulating flow resistance in the porous media. Later in this paper, the model's validity will be discussed by making a comparison between the theory and the laboratory data.

In order to roughly estimate the discharge computation error ΔQ_ε, we assume the minimum value ε=0.0005 ($\mathrm{m}^6/\mathrm{sec}^2$) by referring to Fig. 5. Here, ΔQ_ε becomes

$$\Delta Q_\varepsilon = \{\varepsilon/(M_K+M_O)\}^{1/2} = (0.0005/345)^{1/2} (\mathrm{m}^3/\mathrm{sec}) = 0.0012\ (\mathrm{m}^3/\mathrm{sec}) \tag{23}$$

This is not as small as the discharge range in the K-Flume experiment, but is within the data scattering in the O-Flume experiment. The main reason for such a relatively large value of ΔQ_ε is the uncertainty of discharge measurement in the O-Flume. As discussed later, the computation error for the K-Flume experiment is about ten times smaller than the average error given above. Despite the experimental errors, the following sections

show that computation using the identified coefficients (e, f) provides a certain accuracy of discharge estimation within the data scattering.

DEPENDENCY OF DISCHARGE ON RELATING HYDRAULIC PARAMETERS

Reynolds Number Effect (Scale Effect)

The flow resistance consists of the laminar and turbulent flow components as formulated in Eq. (10). The effect of fluid viscosity or the physical model's scale can be measured by examining the functional relationship between discharge and Reynolds number R_e.

In Fig. 6, the normalized discharge F_0 is plotted against the non-dimensional flow depth h_0/L and R_e for the cases of $\Delta h/h_0$=0.2 and d_m/h_0=0.2. The experimental data points plotted in symbols are very limited under the fixed conditions of $\Delta h/h_0$ and d_m/h_0. The curves are a theoretical estimation. Some laboratory data show poor agreement with the theoretical solutions. There are several possible reasons for the errors. The open channel flow in the experiment is not completely uniform both on the upstream and downstream sides of the weir, while uniform flows are assumed in the analysis. This may result in a discrepancy in the water depth evaluation between the experiment and the theory. Errors in discharge measurement may also arise, especially in the O-Flume, as previously discussed. In addition, uncertainty included in the coefficients (e, f) may result in prediction errors. However, it is very difficult to determine which factor is predominant in producing errors.

Nevertheless, both theory and experiment show that discharge F_0 increases as R_e increases, and asymptotically approaches a constant value that is given independently of R_e. This asymptotic dependency of F_0 on R_e suggests that Reynolds number or fluid viscosity has less influence on the through-flow discharge for larger Reynolds numbers. The figure indicates that $R_e \cong 5{,}000$ is the lower limit above which discharge is scarcely influenced by the Reynolds number. In order to further investigate the viscous effect on the flow property, the fraction of laminar to total flow resistance, i.e. $D_L/(D_T+D_L)$, is plotted against R_e in Fig. 7, where D_L and D_T are defined in Eq. (10). The figure confirms that the laminar flow component D_L has less influence on the total flow resistance (D_T+D_L) as R_e increases. In other words, the total flow resistance consists mostly of turbulent flow component D_T in the range of a large Reynolds number. This figure confirms that $R_e \cong 5{,}000$ is again a Reynolds number threshold that divides the flow regime into a viscosity-dominant zone and a turbulence-dominant zone. Summarizing the results from Figs. 6 and 7, it can be concluded that the scale effect or fluid viscosity is negligibly small, and the flow becomes independent of R_e in a range of R_e>5000.

Here, it should be noted that the weir length L is involved in the parameter h_0/L in these relationships. As

the weir length L decreases or the ratio h_0/L increases, the flow rate F_0 increases.

Effect of Bed Slope *i*

The hydraulic gradient inside the weir may be much greater than the bed slope i, except in the case of very steep slope channels. In order to confirm that the bed slope has little influence on the discharge, F_0 is plotted against h_0/L in Fig. 8(a) for a varied bed slope i. In addition, Fig. 8(b) shows a functional relationship between F_0 and i, for varying water depth h_0/L. Since the data points satisfying the conditions d_m/h_0=0.2 and $\Delta h/h_0$=0.2 are very limited, it is difficult to find a functional dependency only from the plotted laboratory data. Instead, the theoretical curves help us to understand effect of the bed slope i on the discharge. The theoretical curves in Fig. 8(a) are drawn so closely together that one can hardly distinguish each curve. Fig. 8(b) is a direct description for a functional dependency of F_0 on i, which shows that F_0 asymptotically approaches a constant value with decreasing i. Fig. 8 shows that the discharge is almost independent of bed slope in the range of i<1/100.

Effect of Backwater

The downstream flow depth h_3 or the flow depth difference between the up- and downstream sides of the weir, $\Delta h(=h_0-h_3)$, may be a parameter for measuring the backwater effect. It is thought that the smaller the depth difference Δh, the more predominant the backwater effect becomes, and thus the flow rate decreases. This tendency is confirmed in Fig. 9, which shows a functional relationship between F_0 and h_0/L for varied water level difference $\Delta h/h_0$. The experimental result showing that F_0 decreases as $\Delta h/h_0$ decreases is estimated by the theoretical curves.

Since the S-Flow is downstream-controlled, the flow rate is eventually dependent on the parameter $\Delta h/h_0$, as shown in the figure. On the other hand, discharge of the C-Flow is determined solely by the critical depth h_C that occurs at the control section $x=L^-$ in the case when $\Delta h/h_0$ is large enough. In the latter case, the discharge becomes independent of $\Delta h/h_0$, as written in Eq. (20) and confirmed in Fig. 9. The S-Flow asymptotically approaches the C-Flow in the extreme of $h_2 \rightarrow h_C$ or $\Delta h \rightarrow \Delta h_C$, where $\Delta h_C=(h_{3C}- h_C)$ and h_{3C} is a value of h_3 when h_2 is equated to h_C in Eq. (19). This asymptotic tendency is also confirmed in Fig. 9.

DISCHARGE RELATIONSHIP

Example of Discharge Curve Q~h_0

In engineering practice, a functional relationship between the discharge Q and the water level h_0, the so-called “discharge-curve”, is required when designing a weir. Examples of the curve are shown in Fig. 10 for

the case of d_m/h_0=0.38. The theoretical discharge computed from the present analysis correlates well with the experimental data.

Correlation between Theoretical and Experimental Discharge

The solution for discharge Q_{TH} was computed for all the experimental runs and compared with the experimental values Q_{EX} to verify the correlation between the theory and the experiment. As shown in Fig. 11, the theoretical estimation Q_{TH} is in excellent agreement with the experimental data points Q_{EX} in the range of Q<0.003m/sec^3. Data plotted in this range are mostly from the K-Flume. On the other hand, in the range of Q>0.003m/sec^3, the estimation error is not so small. There are two possible reasons for the poor agreement between Q_{EX} and Q_{TH}. The first reason may be the uncertainty of discharge measurement in the O-Flume, as previously discussed. The second one may be the dependency of the coefficients (e, f) on structural parameters of the porous media, although they are treated as constant in the present analysis. If the first reason is the main reason, the present model is thought to provide a reasonable estimation for a wide range of discharge, since the theoretical solution passes through the center of data scattering. On the other hand, for cases when the error is caused by the second reason, a different version of flow resistance law, such as the capillary model proposed by Legrand (2002), should be adopted in the analysis. Even in this case, most formulations in the present flow analysis, except in the modelling of flow drag force, will be kept unchanged. Since there is still sensitivity of the present solution with respect to (e, f), it is worthwhile to further examine the flow resistance to improve discharge analysis.

CONCLUDING REMARKS

In order to use a rubble-mound weir as a water storage facility, discharge through the weir was evaluated by performing one-dimensional analysis and a laboratory experiment. The governing parameters were water depths on the up- and downstream sides of the weir, length and porosity of the weir, average diameter of the rubble mound and bed slope. The analysis provided a solution for discharge as a function of the governing parameters. The functional dependency of discharge on each parameter was in agreement with laboratory data, although the flow resistance should be further investigated and the hydraulic measurement has to be improved. The main findings are summarized below.

Dimensionless discharge F_0 is an increasing function of the dimensionless water depth h_0/L upstream of the weir, the specific flow depth difference between upstream and downstream of the weir $\Delta h/h_0$, the dimensionless

diameter of the rubble mound materials d_m/h_0 and the bed slope i. The effect of the bed slope i is negligibly small in the range of $i<1/100$. When the Reynolds number R_e is greater than about 5,000, the discharge is almost free from scale effect, and the laminar flow component has little effect on the flow rate. This suggests that the laminar flow component of flow resistance can be neglected in computing discharge through a prototype rubble mound weir. Although the functional dependency of discharge on the governing parameters is mostly described by the analysis, there still remains uncertainty in the model coefficients (e, f). In order to refine the model's performance, it is worthwhile to test another version of flow resistance law, such as the capillary model.

Using the current theory, we can make a suitable design for a rubble mound weir under given river channel conditions. It is necessary to further investigate other aspects of the rubble mound weir, such as dynamic stability against flow force, aeration rate of the weir, feasibility of the longitudinal migration of aquatic life, sedimentation of suspended solids in weir pores, etc.

APPENDIX I. REFERENCES

Ahmed, N., and Sunada, D. K. (1969). “Nonlinear flow in porous media.” *J. Hydr. Div.*, ASCE, 95(6), 1847-1857.

Antohe, B. V., and Lage, J. L. (1997). “A general two-equation macroscopic turbulence model for incompressible flow in porous media.” *Int. J. Heat Mass Transfer*, 40(13), 3013-3024.

Arbhabhirama, A., and Dinoy, A. A. (1973). “Friction factor and Reynold’s number in porous media flow.” *J. Hydr. Div.*, ASCE, 99(6), 901-911.

Bari, R., and Hansen, D. (2000). “Analyzing flow through mine waste dumps.” *Proc. 7th Int. Conf. on Tailings and Mine Waste*, Balkema, Fort Collins, Colorado, USA, 231-241.

Basak, P. (1976). “Steady non-Darcian seepage through embankments.” *J. Irrig. and Drainage Div*., ASCE, 103(4), 435-443.

Basak, P. (1977). “Non-Darcy flow and its implications to seepage problems.” *J. Irrig. Drainage. Div.*, ASCE, 103(4), 459-473.

Chan, E. C., Fue-Sang, L., and Yovanovich, M. M. (2000). “Numerical study of forced flow in a back-step channel through porous layer.” *Proc. NTHC'00, 34th ASME National Heat Transfer Conference*, ASME, NHTC2000-12118, Pittsburgh, Pennsylvania, USA, 1-6.

Chow, V. T. (1959). *Open Channel Hydraulics*, McGraw-Hill Book Company, New York.

Comiti, J., and Renaud, M. (1989). “A new model for determining mean structure parameters of fixed bed from pressure drop measurements: application to beds packed with parallelepipedal particles.” *Chemical Engrg. Sci.*, 44(7), 1539-1545.

Curtis, R. P., and Lawson, J. D. (1967). “Flow over and through rockfill banks.” *J. Hydr. Div.*, ASCE, 93(5), 1-21.

French, R. H. (1986). *Open Channel Hydraulics*, McGraw-Hill Book Company, New York.

Garga, V. K., Hansen, D., and Townsend, R. D. (1995). “Mechanism of massive failure for flow through rockfill embankments.” *Can. Geotech. J*., 32(6), 927-938.

George, G. H., and Hansen, D. (1992). “Conversion between quadratic and power law for non-Darcy flow.” *J. Hydraulic Engrg.*, ASCE, 118(5), 792-797.

Hansen, D., Garga, V. K., and Townsend, D. R. (1994). “Selection and application of a one-dimensional non-Darcy flow equation for two-dimensional flow through rockfill embankments.” *Can. Geotech. J*., 32(2), 223-232.

Hansen, D., and Bari, R. (2002). “Uncertainty in water surface profile of buried stream flowing under coarse material.” *J. Hydraulic Engrg.*, ASCE, 128(8), 761-773.

Legrand, J. (2002). “Revisited analysis of pressure drop in flow through crushed rocks.” *J. Hydraulic Engrg.*, ASCE, 128(11), 1027-1031.

Li, B., Garga, V. K., and Davies, M. H. (1998). “Relationships for non-Darcy flow in rockfill.” *J. Hydraulic Engrg.*, ASCE, 124(2), 206-212.

Mustafa, S., and Rafindadi, N. A. (1989). “Nonlinear steady state seepage into drains.” *J. Irrig. Drainage Engrg.*, ASCE, 115(3), 358-376.

Parkin, A. K., Trollope, D. H., and Lawson, J. D. (1966). “Rockfill structures subject to water flow.” *J. Soil Mech. Foundation . Div.*, ASCE, 92(6), 135-151.

Samani, H. M. V, Smani, J. M. V., and Shaiannejad, M. (2003). “Reservoir routing using steady and unsteady flow through rockfill dams.” *J. Hydraulic Engrg*., ASCE, 129(6), 448-454.

Shimizu, Y., Tsujimoto, T. and Nakagawa, H. (1990). “Experiment and macroscopic modeling of flow in high permeable porous medium under free-surface flow.” *J. Hydroscience and Hydraulic Engineering*, Japan Soc. Civ. Eng., 8(1), 69-78.

Stephenson, D. (1979). *Rockfill in hydraulic engineering*, Elsevier Scientific, Amsterdam.

Thiruvengadam, M. and Kumar, G. N. P. (1997). “Validity of Forchheimer Equation in Radial Flow through Coarse Granular Media.” *J. Engrg. Mech.*, ASCE, 123(7), 696-705.

Todd, D.(1960). *Hydrogeology*, McGraw-Hill, New York.

Trussell, R. R., and Chang, M. (1999). “Review of flow through porous media as applied to head loss in water filters.” *J. Environ. Engrg*. ASCE, 125(11), 998-1006.

Ulrich, T. (1987). “Stability of rock protection on slopes.” *J. Hydr. Div.*, ASCE, 113(7), 879-891.

Vafai, K. (2000). *Handbook of Porous Media*, Marcel Dekker, Inc., New York.

Venkataraman, P., and Rama Mohan Rao, P. (1998). “Darcian, transitional, and turbulent flow through porous media.” *J. Hydraulic Engrg*., ASCE, 124(8), 840-846.

Venkataraman, P., and Rama Mohan Rao, P. (2000). “Validation of Forchheimer’ law for flow through porous media with converging boundaries.” *J. Hydraulic Engrg*., ASCE, 126(1), 63-71.

Volker, R. E. (1969). “Nonlinear flow in porous media by finite elements.” *J. Hydr. Div.*, ASCE, 95(6), 2093-2114.

Volker, R. E. (1975). “Solutions for unconfined non-Darcy seepage.” *J. Irrig. Drainage Div*., ASCE, 101(1),

53-65.

Ward, J. C. (1964). “Turbulent flows in porous media.” *J. Hydr. Div.*, ASCE, 90(5), 1-12.

ACKNOWLEDGEMENTS

This study was financially supported by the Grant in Aid for Scientific Research, from Japan Ministry of Education in 2000-2003 (Project number: 12650513 and 14350268, Project leader: Kohji MICHIOKU). The laboratory experiment was conducted under the coorporation of Mr. S.Yamasawa, an undergraduate student from Kobe University and Mr. T.Oonishi and Mr.S.Morinaga, graduate students from Okayama University.

APPENDIX II. NOTATION

The following symbols are used in this paper:

(A_1, A_2) = coefficients in a quadratic type flow resistance law;

A_3 = an proportional coefficient in a power type flow resistance law;

B_0 = channel width [Fig.3(c)];

B_1 = channel width at the contracted section [Fig.3(c)];

b_k = pore width in a complex Hele-Shaw system [Fig.3(b)];

c = model coefficient for drag force of rubble mound material [Eq.(3)];

D_L = laminar flow components of the flow resistance in the rouble mound;

D_T = turbulent flow components of the flow resistance in the rouble mound;

d_m = mean diameter of the rubble mound material;

e = proportional coefficients regarding to the parameters c [Eq.(5)];

F_0 = upstream Froude number or normalized discharge defined as $F_0=q/(gh_0^3)^{1//2}$;

f = proportional coefficients regarding to the parameters K [Eq. (4)];

g = gravitational acceleration;

h_j = water depths at the cross sections j=0,1,2 and 3 that corresponds to $x=0^-$, 0^+, L^- and L^+, respectively [Fig.2];

h' = transition water depth between the cross sections $x=0^-$ and 0^+;

h" = transition water depth between $x=L^-$ and L^+

h_C = critical water depth occurring at $x=L^-$;

I = hydraulic gradient;

i = bed slope of the channel;

K = permeability or model coefficient scaling the gravel mean diameter d_m [Eq.(3)];

L = length of the rubble mound weir;

l = non-dimensional weir length defined as L/h_0;

l_w = a characteristic length scale of porous media;

M = number of experimental runs;

M_K = subtotal number of experimental runs in the K-Flume experiment;

M_O = subtotal number of experimental runs in the O-Flume experiment;

N = total number of pores in a complex Hele-Shaw system [Fig.3(b)];

n = porosity of the weir;

Q = volumetric discharge or flow rate;

Q_{EX} = discharge in the experiment;

Q_{TH} = theoretical solution of discharge;

q = discharge per unit width;

R_e = Reynolds number defined by $R_e = q/\nu$;

R_w = Reynolds number defined by $R_w = Vl_w/\nu$;

U_0 = mean velocity at the upstream of the weir or $x = L^-$, which is defined as $U_0=(Q/B_0h_0)$ [Fig. 3(c)];

U_1 = mean velocity at the downstream side of the section (I) or $x = L^+$, which is defined as $U_1=(Q/B_1h_1)$;

U_S = apparent velocity in the porous body defined by q/h;

V = a bulk velocity in a porous media;

W = an exponent in a power type flow resistance law for non-Darcian flow;

x = longitudinal coordinate originated at the upstream boundary of the weir;

γ_j = dimensionless water depth defined by $\gamma_j=h_j/h_0$;

Δh = water level difference between the up- and down-stream sides of the weir, (h_0-h_3);

ΔQ_ε = error or accuracy of discharge computation;

$(\delta_1,\delta_2, \delta_3)$ = velocity correction factors;

λ = width ratio or two-dimensional porosity in a suddenly contracted channel system defined by $\lambda=B_1/B_0$;

ν = kinematic viscosity of water;

ρ = density of water;

Ω_C = function for C-flow discharge [Eq.(20)];

Ω_S = function for S-Flow discharge [Eq.(21)].

subscripts

j = positive integer indices, where j=0,1,2 and 3 corresponds to values at $x=0^-$, 0^+, L^- and L^+, respectively;

m = an experimental run number ranging between m=1,2, $\cdots M_K+M_O$.

Table 1 Experimental conditions for K-Flume experiment.

Reynolds number: R_e=250~4,000, Froude number F_0=0.008~0.055, Porosity: n=0.32,0.37				
d_m (mm) (1)	L (cm) (2)	i (3)	Q (m^3/s) $\times 10^{-3}$ (4)	M (5)
19.1	30	1/200	0.481-1.56	24
		1/800	0.387-1.43	22
		1/1,600	0.522-1.39	23
34.6	30	1/200	0.370-1.55	24
		1/800	0.246-1.72	22
		1/1,600	0.231-1.54	23
19.1	75	1/200	0.168-0.945	18
		1/800	0.160-0.735	18
		1/1,600	0.159-0.810	18
34.6	75	1/200	0.193-1.16	18
		1/800	0.255-0.988	18
		1/1,600	0.285-0.817	18
Total number of experimental runs M_K				246

Notation
d_m: Average grain diameter , L: Weir length,
i: Bed slope, Q: T,otal discharge,
M is the number of experimental run

Table 2 Experimental conditions for O-Flume experiment.

Reynolds number: R_e=5,000~18,000, Froude number F_0=0.01~0.07, Porosity: n=0.37, 0.38				
d_m (mm) (1)	L (cm) (2)	i (3)	Q (m^3/s) $\times 10^{-3}$ (4)	M (5)
19.5	30	1/400	2.13-6.41	24
41.0	30		1.64-5.88	27
19.5	60		2.10-6.02	23
41.0	60		2.21-5.95	25
Total number of experimental runs M_O				99

Notation
d_m: Average grain diameter , L: Weir length,
i: Bed slope, Q: T,otal discharge,
M is the number of experimental run

FIGURE CAPTIONS

Fig.1 A rubble mound weir (Johbaru River, Japan)

Fig.2 Model system and definition of variables

Fig.3 Analogy among (a) rubble mound system, (b) a Hele-Shaw system and (c) a sudden contraction system; plane views of flow

Fig.4 Cumulative size-distribution curves for the granular materials

Fig.5 Contours of ε in the (e, f) plane and determination of the optimum pair of (e, f).

Fig.6 Dependency of normalized discharge F_0 on Reynolds number R_e ($\Delta h/h_0$=0.2, d_m/h_0=0.2).

Fig.7 Ratio of laminar flow resistance to total flow resistance, $D_L/(D_T+ D_L)$.

Fig.8 Dependency of F_0 on bed slope i ($\Delta h/h_0$=0.2, d_m/h_0=0.2).

Fig.9 Functional relationship between F_0 and h_0/L plotted for varied water level difference $\Delta h/h_0$ (d_m/h_0=0.2).

Fig.10 Examples of discharge curve; plotting of Q against h_0 for the case of d_m/h_0=0.38.

Fig.11 Correlation of theoretical discharge Q_{TH} with the experimental one Q_{EX} for all the data points

Fig.1　A rubble mound weir (Johbaru River, Japan)

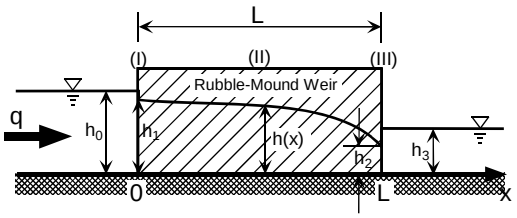

Fig.2 Model system and definition of variables

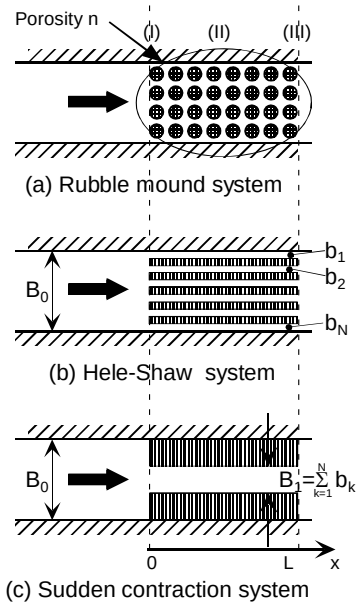

Fig.3 Analogy among (a) rubble mound system, (b) a complex Hele-Shaw system and (c) a sudden contraction system; plane views of flow

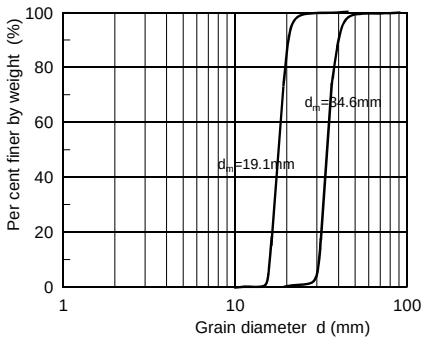

Fig.4 Cumulative size-distribution curves for the granular materials

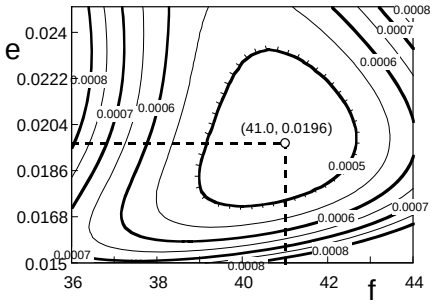

Fig.5 Contours of ε in the (*e*, *f*) plane and determination of the optimum pair of (*e*, *f*).

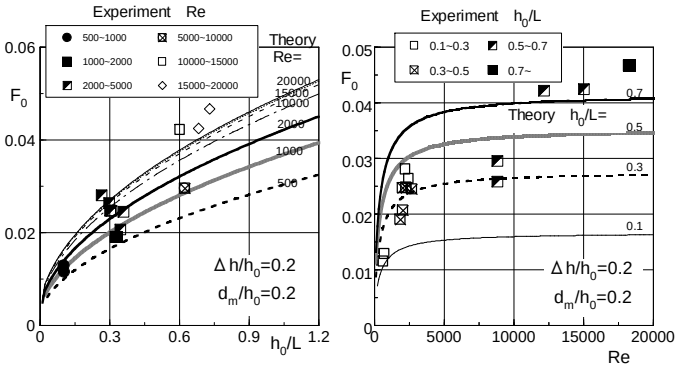

(a) F_0 versus h_0/L (b) F_0 versus R_e

Fig.6 Dependency of normalized discharge F_0 on Reynolds number R_e ($\Delta h/h_0$=0.2, d_m/h_0=0.2).

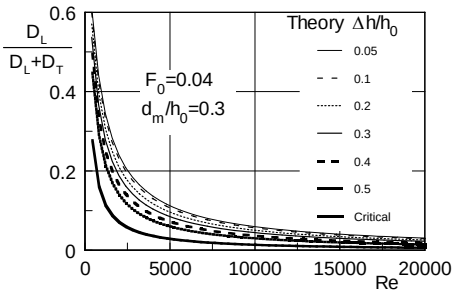

Fig.7 Ratio of laminar flow resistance to total flow resistance, $D_L/(D_T+ D_L)$.

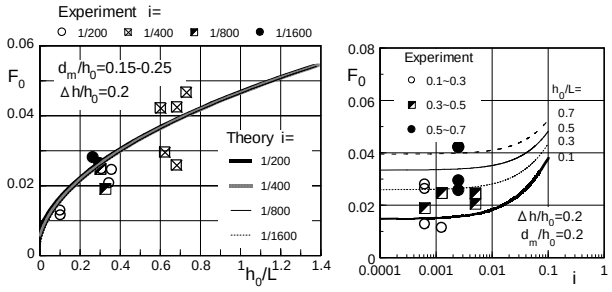

(a) F_0 versus h_0/L (b) F_0 versus i

Fig.8 Dependency of F_0 on bed slope i ($\Delta h/h_0$=0.2, d_m/h_0=0.2).

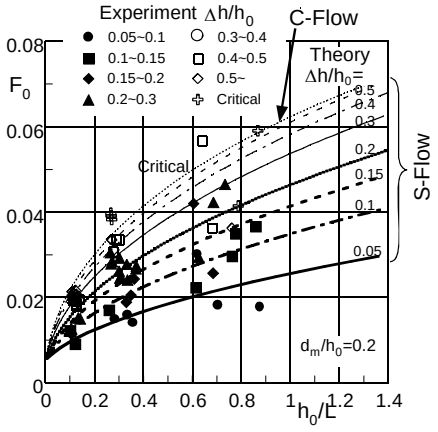

Fig.9 Functional relationship between F_0 and h_0/L plotted for varied water level difference $\Delta h/h_0$ (d_m/h_0=0.2).

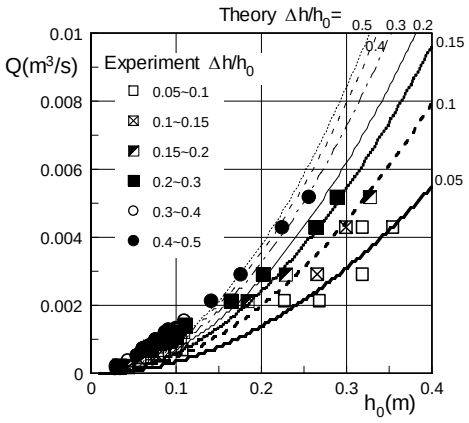

Fig.10 Examples of discharge curve; plotting of Q against h_0 for the case of d_m/h_0=0.38.

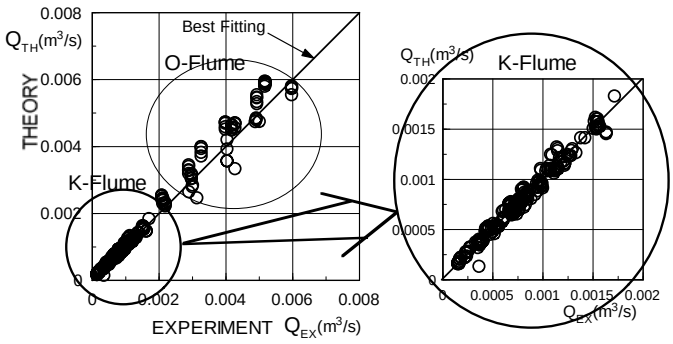

(a) All data points (b) Data from the K-Flume

Fig.11 Correlation of theoretical discharge Q_{TH} with the experimental one Q_{EX} for all the data points.